# Molecular Dynamics Simulations on Crystallization of Polyethylene Copolymer with Precisely Controlled Branching

**Xiu-bin Zhang,† Ze-sheng Li,* Hua Yang, and Chia-Chung Sun**

*Institute of Theoretical Chemistry, State Key Laboratory of Theoretical and Computational Chemistry, Jilin University, Changchun 130023, People's Republic of China*

*Received January 6, 2003; Revised Manuscript Received December 1, 2003*

ABSTRACT: Molecular dynamics simulations of three kinds of linear low-density polyethylene (LLDPE) single-chain models with precisely controlled branching are performed. It is shown that the crystallinity of copolymers with branches shorter than $C_{10}H_{21}$ decreases with increasing branch length, whereas for copolymers having branches longer than $C_{10}H_{21}$, the crystallinity increases as the branch length increases. From the simulations of ethylene/vinyl chloride copolymer model, it is found that the crystallization process and driving force of LLDPE chain with polar comonomer are similar to those having a nonpolar comonomer, and the MD simulations of the models with branches of different flexibilities show that as branch flexibility decreases, the side-chain co-crystallization becomes more difficult, and the corresponding lamella is packed more loosely.

## I. Introduction

For polymer materials, especially for polymers with regular chain structure, polymer crystallization is a general phenomenon and is a very important process in industry. It controls the structural formation of the polymer chain and thereby dominates the properties of the final products.[1] Obtaining the relationship between the crystal structure and properties of polymers will be very helpful for improvement of existing polymer materials and development of new ones. To obtain the relationship, it is necessary to understand and reveal the dynamic behavior and mechanism of polymer crystallization at the molecular level. However, due to the multiformity of polymer crystallization, it seems very difficult to study systematically the crystal properties of polymer materials at the molecular level by present experimental techniques. Recently, molecular dynamics (MD) simulation has been proved to be a powerful tool for investigating the microscopic dynamics behavior and mechanism of polymer crystallization.[2−15]

Linear low-density polyethylene (LLDPE), which has gradually gained commercial acceptance in various applications for its superior mechanical properties, is a copolymer of ethylene and an α-olefin. Many experimental investigations[16−31] have been carried out to study the relationship between microstructures and crystal properties of the copolymer. It is known that the crystallinity of LLDPE influences the final properties of the polymer and is affected by molecular weight, comonomer type, concentration of branches, and their distribution along the copolymer backbone. To fully understand the crystallization behavior of the branched molecules, more homogeneous fractions of the copolymer are needed. However, the LLDPE samples normally have a heterogeneous microstructure. This makes it difficult to get experimentally more homogeneous fractions to systematically investigate the crystallization behavior of the branched molecules. Recently, ethylene copolymers with precisely controlled methyl branching have been created by use of acyclic diene metathesis (ADMET) chemistry as the mode of polymerization,[32,33] which will provide a basis for better understanding of the morphology, crystalline structure, and thermodynamics of the crystallization process of the copolymer. But to our knowledge, information about the morphology and crystalline structure of the copolymer with well-controlled branching has not been reported experimentally up to now.

On the other hand, although the effect of comonomer type (branch length) on melting and crystallization properties of LLDPE has been intensively studied,[26−31] it is still a topic of controversy. In the experimental study of Kim and Phillips,[31] it was reported that there is a branch effect on melting temperature depression: the melting temperature depression of ethylene/1-octene random copolymers with hexyl branches was significantly larger than those of ethylene/1-butene and ethylene/1-propene copolymers having ethyl and methyl branches, respectively. However, Alamo et al.[29,30] found that the thermodynamic properties of a series of random ethylene copolymers with 1-butene, 1-hexene, or 1-octene as comonomers were independent of the chemical nature of the counit or branch group. In experimental investigation of melting points of copolymers of ethylene and 1-alkenes ranging from 1-butene to 1-octadecene, Clas et al.[27] pointed out that melting points determined by differential scanning calorimetry were independent of branch length at low comonomer contents; however, at higher comonomer contents (5−9 mol % 1-alkene), melting points decrease in the order 1-butene > 1-octene > 1-octadecene copolymers.

Recently, Doran and Choi[34] carried out MD simulations to study the effects of branch length, branch content, and branch distribution on the crystalline structure of LLDPE at 300 K. But in their models the branch length is only up to 6 carbons. So it seems necessary to further study the effect of branch length on the crystallinity of LLDPE, which is one of the issues of this paper. As further extensions of our previous studies,[35,36] the temperature effect on the crystallinity of LLDPE, the crystallization of co-polyethylene with

* Corresponding author: e-mail zeshengli@mail.jlu.edu.cn.
† Present address: Department of Chemistry and Cherry L. Emerson Center for Scientific Computation, Emory University, Atlanta, GA 30322.

10.1021/ma030010v CCC: $27.50 
Published on Web 08/17/2004

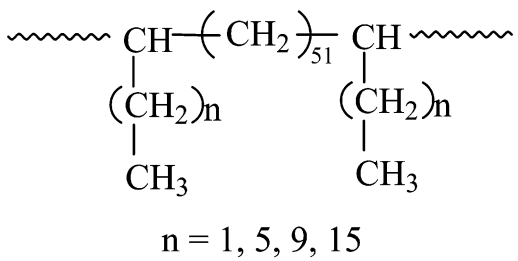


**Figure 1.** Schematic representation of the copolymer chain models with precisely controlled alkyl branching.

**Table 1. Copolymer Chain Models with Precisely Controlled Alkyl Branching**

| notation | branch length (carbons) | $CH_x$ units in backbone ($x$ = 1, 2) | α-olefin monomer (%) | simulation time[a] (ns) isotherm | simulation time[a] (ns) nonisotherm |
|---|---|---|---|---|---|
| pe-51-b2 | 2 | 500 | 3.85 | 8 | 15 |
| pe-51-b6 | 6 | 500 | 3.85 | 8 | 15 |
| pe-51-b10 | 10 | 500 | 3.85 | 8 | 15 |
| pe-51-b16 | 16 | 500 | 3.85 | 8 | 15 |

[a] For isothermal and nonisothermal crystallization.

polar monomer, and the effect of branch flexibility on side-chain crystallization are also investigated.

## II. Models and Simulation Methods

Three kinds of LLDPE chain models—with alkyl branches (such as ethyl, hexyl, $C_{10}H_{21}$, or $C_{16}H_{33}$ branches), with chlorine atom branches, and with $C_{16}H_{33}$ branches but in which different numbers of C=C double bonds are involved—are used for the MD simulations. Each model has 500 $CH_x$ ($x$ = 1, 2) units in the chain backbone and 3.85 mol % comonomer (10 branches). Along the main chain the branches are regularly distributed (i.e., there are equal numbers of $CH_2$ units between any two given branches). The three kinds of chain models are denoted as pe-51-b$n$ ($n$ = 2, 6, 10, or 16), pe-51-Cl, and pe-51-b16-$m$ ($m$ = 1−3), respectively, where 51 means that there are 51 $CH_2$ units between any two given branches, $n$ represents the number of carbon atoms in a branch, Cl represents a chlorine atom, and $m$ represents the number of C=C double bonds in a $C_{16}H_{33}$ branch. For brevity, only the schematic representations of pe-51-b$n$ models are depicted in Figure 1.

In the simulations, a random coil of each chain model is created first, and then the random coil is annealed 10 cycles from $T$ = 300 to 1000 K and cooled to 300 K at intervals of 50 K/0.1 ps to overcome local minimum energy barriers. At the end of each cycle, the structure is relaxed by minimization. From the fully relaxed structure, the canonical Nosé−Hoover molecular dynamics simulations are performed. The integration time step is set to 0.001 ps, the temperature is set to $T$ = 300 K, and a relaxation constant for the heat bath variable is 0.1 ps. The cutoff distance for the van der Waals interaction is 10.5 Å. The duration of the simulation for each model is 8 ns. To investigate the effect of temperature on the LLDPE crystallization, we also carried out MD simulations of the chain models with alkyl branches from $T$ = 650 K cooled stepwise to $T$ = 300 K at a rate of 25 K/ns. The total duration of the simulations is about 15 ns (as listed in Table 1).

Following our previous studies,[35,36] in the present simulations, the Dreiding II force field[37] is used, and the united atom approximation is adopted to simplify the calculations. The total potential energy $E_{total}$ consists of four parts: (1) the bond-stretching energy $E_{stretch}$ for two adjacent united atoms, (2) the bond-bending energy $E_{bend}$ among three adjacent united atoms, (3) the torsion energy $E_{torsion}$ among four adjacent united atoms, and (4) the 12-6 Lennard-Jones potential $E_{vdW}$ between two nonbonded atoms. The total potential energy $E_{total}$ can be expressed as

$$\begin{aligned} E_{total} &= E_{bond} + E_{vdW} \\ &= E_{stretch} + E_{bend} + E_{torsion} + E_{vdW} \\ &= \frac{1}{2}K_b(R - R_0)^2 + \frac{1}{2}K_\theta(\theta - \theta_0)^2 + \\ &\qquad \frac{1}{2}K_\phi[1 - d\cos(3\phi)] + D_0\left[\left(\frac{\sigma}{r}\right)^{12} - 2\left(\frac{\sigma}{r}\right)^{6}\right] \end{aligned} \quad (1)$$

where $R$ is the bond length between two adjacent atoms, $R_0$ is the equilibrium bond length, $\theta$ is the bond angle between three adjacent atoms, $\theta_0$ is the equilibrium angle, $\phi$ is the dihedral angle formed by four consecutive atoms, and $r$ is the distance between two nonbonded atoms. It should be noted that, due to the polar vinyl chloride comonomers that are contained in the pe-51-Cl copolymer chain model, the coulombic interaction between two nonbonded atoms of the polymer chain should not be ignored. So in the simulation of ethylene-*co*-vinyl chloride copolymer, the coulombic interaction energy between two nonbonded atoms $E_{coulomb}$ is added to $E_{total}$ of the system. The functional form of $E_{coulomb}$ is expressed as

$$E_{coulomb} = C_0 \sum_i \sum_{j>i} \frac{Q_i Q_j}{\epsilon R_{ij}} \quad (2)$$

where $\epsilon$ is the dielectric constant, $Q_i$ and $Q_j$ are the partial charges, $R_{ij}$ is the distance between atoms $i$ and $j$, and $C_o$ is a conversion factor employed to yield Coulombic interaction energy in units of kilocalories per mole.

The random coil of pe-51-Cl is annealed from 300 to 1000 K and cooled to 300 K at intervals of 50 K repeatedly. At the end of each cycle, the structure is relaxed by minimization and the charge equilibration (QEq) [38] is followed. The QEq method is chosen because it allows the charges to respond to changes in the environment, including those in applied fields, and can be applied to any material (polymer, ceramic, semiconductor, biological, metallic).[38] From the fully relaxed structure after the charge equilibration, the NVT MD simulation starts at 300 K.

## III. Results and Discussion

We found in previous studies that the morphology of the lamella originating from the random coil was generally similar to that from an all-trans stretched chain.[35,36] So in this study, we only performed MD simulations starting from random coils of the three kinds of LLDPE chain. The results will be discussed in the following four subsections. In sections A and B, the results of isothermal and nonisothermal crystallization of LLDPE chain with alkyl branches are given, respectively, and the effects of branch length and temperature on the crystallinity of the copolymer are investigated. In section C the crystallization of the LLDPE chain with a polar comonomer is studied. Finally, the effect of branch flexibility on side-chain crystallization is discussed in section D.

**A. Isothermal Crystallization of LLPDE Chain with Alkyl Branches.** In our previous simulations,[35] we studied the crystallization process of LLPDE chain with methyl branches. To gain further understanding of the crystallization behavior of the LLDPE molecule, now let us discuss the relaxation process of an LLDPE chain with longer alkyl branches. For brevity, we only show the relaxation process of pe-51-b10 chain starting from a random coil at 300 K in Figure 2, where the large black sphere represents a branch site (CH unit) and the small one represents a branch termination group ($CH_3$ unit). It can be seen that the relaxation process of the copolymer chain with $C_{10}H_{21}$ branches has some similarities with that of the polymer chain having methyl

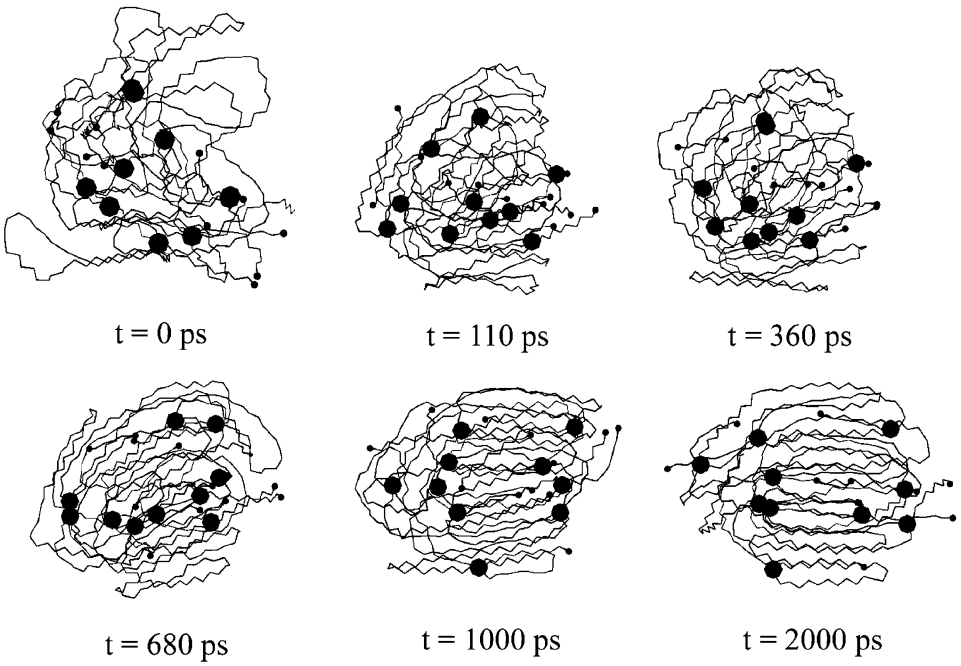


**Figure 2.** Collapse process of pe-51-b10 chain starting from random coil at 300 K, where a large black sphere represents a branch site (CH unit) and a small one represents a termination group of a branch ($CH_3$ unit).

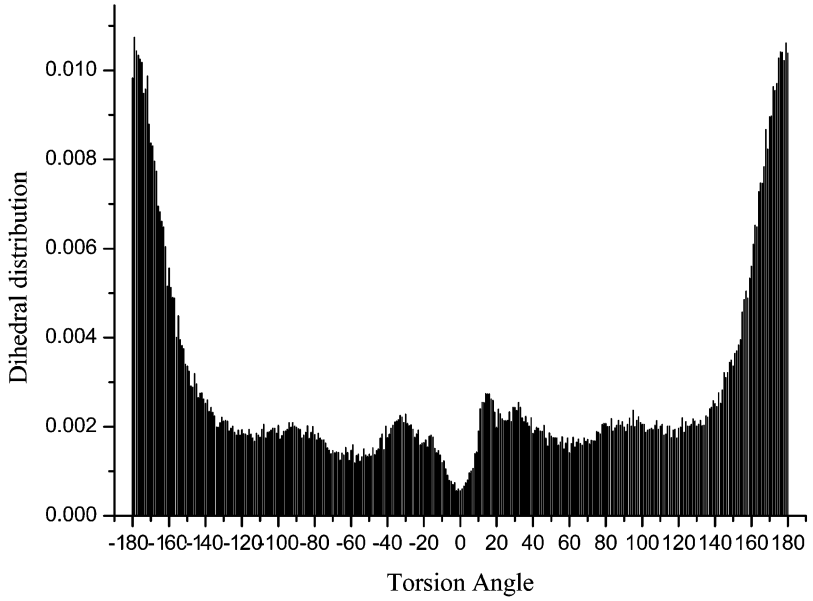


**Figure 3.** Dihedral distributions along pe-51-b10 chain.

branches.[35] What is different is that some $C_{10}H_{21}$ branches are not rejected as methyl branches to the fold surface[35,36] but cocrystallize with the main chain. By comparison with the simulation results of the other three chain models pe-51-b2, pe-51-b6, and pe-51-b16, it is found that ethyl and hexyl branches are all rejected to the amorphous region, whereas most of the $C_{16}C_{33}$ branches cocrystallize with the main chain of pe-51-b16 (as shown in Figure 4). The simulation results confirm our previous conclusions[36] that the branch site (CH unit) is always rejected to the folded surface of the lamellar structure as a defect, while the branch should be considered as a defect with size effect. The critical chain length for side-chain crystallization is 10 carbon atoms.

The dihedral distribution along the pe-51-b10 chain is shown in Figure 3. It is seen that the trans states (dihedrals in regions of $\pm 170° \sim \pm 180°$) are predominant. This characteristic of the conformation of the bonds shows that a lamellar structure (as shown in Figure 4) is formed from a random coil. In the simulation of a single polyethylene chain with 500 $CH_2$ units,[6] it was illustrated that in the bond orientationally ordered structure the gauche states were located exclusively in the fold surface (amorphous region). So it can be concluded that, in a lamellar structure with fixed chain length, the more the trans states are contained, the better the crystallinity of the lamella. Figure 8 shows the fraction of trans state as a function of branch length. The time average is taken between 7500 and 8000 ps for each chain model. From Figure 8, it can be seen that when the branch contains less than 10 carbon atoms, trans states in the corresponding copolymer chain decrease with increasing branch length,[34] whereas when the branch is longer than $C_{10}H_{21}$, the trans states in

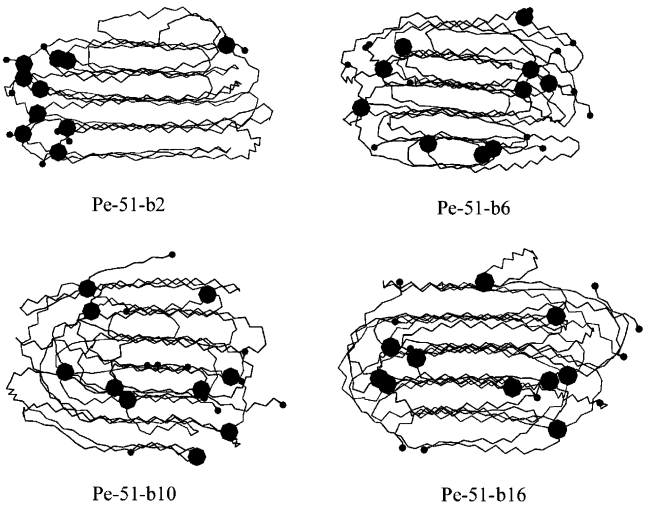


**Figure 4.** Lamellar structures of pe-51-b$n$ ($n$ = 2, 6, 10, or 16) chain models at $t$ = 8000 ps, $T$ = 300 K, where a large black sphere represents a branch site (CH unit) and a small one represents a branch termination group ($CH_3$ unit).

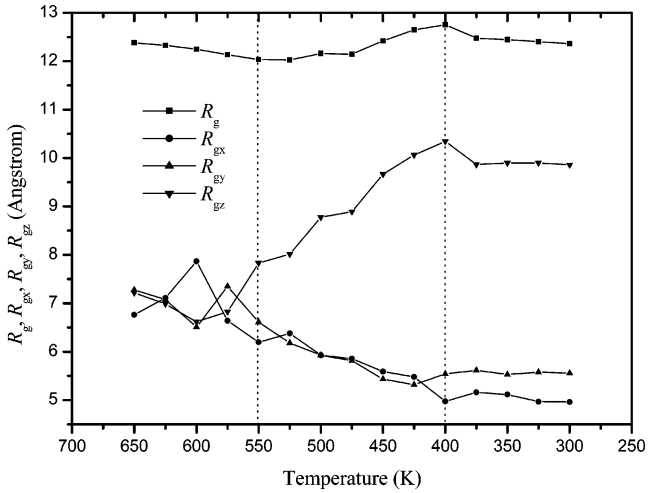


**Figure 5.** Radius of gyration ($R_g$) and its three Cartesian components $R_{gx}$, $R_{gy}$, and $R_{gz}$ of pe-51-b10 chain versus temperature. The time average is taken between 500 and 1000 ps for each temperature.

the corresponding polymer chain increase as the branch length increases. It should be noted that we also obtain one data point with branches of C20. The fraction of the trans state at that point jump to a greater value, but the same trend of fraction of trans state above C10 is preserved.

The result can be visually illustrated by displays of lamellar conformations of the chain models with alkyl branches at 8000 ps in Figure 4. In the corresponding lamellar structure, ethyl and hexyl branches are all located in the amorphous region as defects. And the longer hexyl branches make the amorphous region of pe-51-b6 lamella thicker. However, for the pe-51-b10 model some $C_{10}H_{21}$ branches cocrystallize with the main chain, and many more $C_{16}H_{23}$ branches cocrystallize with the main chain of pe-51-b16. From the results above, it can be found that there is a branch length effect on the crystallinity of LLDPE. For copolymers with branches shorter than $C_{10}H_{21}$, their crystallinity decreases with increasing branch length,[31] whereas for copolymers having branches longer than $C_{10}H_{21}$, their crystallinity increases as the branch length increases.

It should be noted that the above conclusions are limited to the crystallization of copolymer with low branch contents (20 branches/1000 C). It is well-known that the crystallizability of LLDPE is affected by comonomer type, concentration of branches, and their distribution along the polymer backbone. We performed MD simulations of two polymer chain models with higher branch contents (40 $C_{16}H_{33}$ branches/1000 C) but different branch distributions. For the model with precisely controlled branching, a perfect lamellar crystallization is formed, whereas for the model with randomly distributed branching, the overall crystallization of the chain is not so perfect, but it is found that some branches come together and form an ordered region. The result agrees with recent reports of Abusharkh et al.[39] that branches tend to self-assemble at higher branch contents due to the disruption of the lamellar structure of the chain. Since our focus in the present study is on the effects of branch length on the crystallinity of LLDPE, further details of the simulation of chain model with high branch contents are not presented. But it is worthwhile to systematically investigate the effects of branch type and distribution on the crystallization of LLDPE with high branch contents in the future.

**B. Nonisothermal Crystallization of LLPDE Chain with Alkyl Branches.** The radius of gyration $R_g$ and its three Cartesian components $R_{gx}$, $R_{gy}$, and $R_{gz}$, which can be used to characterize the overall shape and orientation of a polymer chain,[6,15] are defined as

$$R_g^2 = \frac{1}{n}\sum_{i=1}^{n}\langle(\mathbf{r}_i - \mathbf{r}_c)^2\rangle \tag{3}$$

$$R_{gx}^2 = \frac{1}{n}\sum_{i=1}^{n}\langle(x_i - x_c)^2\rangle \tag{4}$$

$$R_{gy}^2 = \frac{1}{n}\sum_{i=1}^{n}\langle(y_i - y_c)^2\rangle \tag{5}$$

$$R_{gz}^2 = \frac{1}{n}\sum_{i=1}^{n}\langle(z_i - z_c)^2\rangle \tag{6}$$

where $\mathbf{r}_i = (x_i, y_i, z_i)$ is the position vector of the $i$th atom; $\mathbf{r}_c = (x_c, y_c, z_c)$ is the position vector of the center of mass; $x_i$, $y_i$, and $z_i$ denote the position of the $i$th atom; $x_c$, $y_c$, and $z_c$ denote the position of the center of mass; $\langle ... \rangle$ denotes the ensemble average, and the relation $R_g^2 = R_{gx}^2 + R_{gy}^2 + R_{gz}^2$ holds.

The radius of gyration $R_g$ and its three components $R_{gx}$, $R_{gy}$, and $R_{gz}$ of pe-51-b10 chain at various temperatures are shown in Figure 5. The time average is taken between 500 and 1000 ps for each temperature. From Figure 5 it is found that $R_g$, $R_{gx}$, $R_{gy}$, and $R_{gz}$ vary in three temperature regions, which indicates the relaxation process of pe-51-b10 chain starting from a random coil: (i) At high temperatures (550 K $< T \leq$ 650 K), as the temperature decreases, $R_g$ decreases slightly; however, $R_{gx}$, $R_{gy}$, and $R_{gz}$ are almost constant and equal. This temperature dependence means that the pe-51-b10 chain is in random coil conformation, that is, in melting state. (ii) In the region of 400 K $< T \leq$ 550 K, with decreasing temperature, $R_g$ and its component $R_{gz}$ increase, whereas the other two components $R_{gx}$ and $R_{gy}$ decrease. The result indicates that as the temperature decreases, the random coil of pe-51-b10 chain becomes

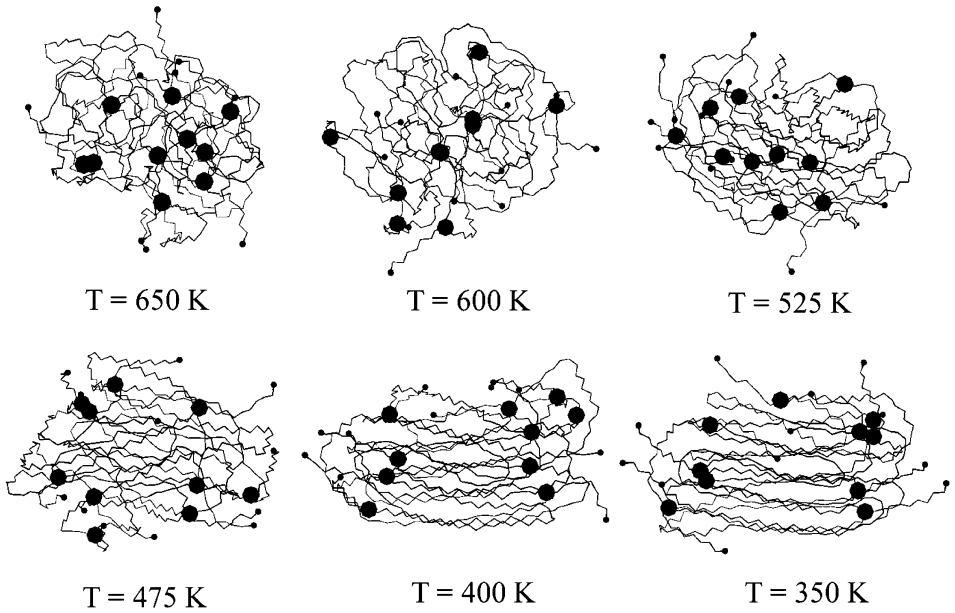


**Figure 6.** Snapshots of the lamellae of pe-51-b10 chain at 1000 ps for various temperatures, where a large black sphere represents a branch site (CH unit) and a small one represents a branch termination group ($CH_3$ unit).

more and more anisotropic and a lamellar structure is formed gradually (as discussed below). (iii) When the temperature is lower than 400 K, $R_g$ and its three components $R_{gx}$, $R_{gy}$, and $R_{gz}$ are almost constant, which shows that the chain conformation does not change with decreasing temperature: the copolymer is in crystal state. From Figure 5, it can also be seen that $R_g$ of the polymer at melt state is nearly equal to that at crystal state, which is supported by transmission electron microscopic (TEM) experiments of Aharoni et al.[40]

The relaxation process of pe-51-b10 random coil during the cooling can be visually illustrated by displays of conformations of the copolymer chain at different temperatures. The snapshots of pe-51-b10 chain conformation at time $t = 1000$ ps for various temperatures are shown in Figure 6. At high temperatures ($T = 650$ and 600 K), the pe-51-b10 chain is in random coil conformation. Comparing the three snapshots at $T =$ 525, 475, and 400 K, we find that the lamellar structures are formed gradually with decreasing temperature, and in the process the branch sites and some of the branches are gradually rejected to the fold surface. At $T = 350$ K, the lamellar structure becomes more perfect, and several branches cocrystallize with the main chain of pe-51-b10.

The lamellar structures of pe-51-b2, pe-51-b6, pe-51-b10, and pe-51-b16 at $t = 1000$ ps and $T = 300$ K, obtained by cooling stepwise at a rate of 25 K/ns, are shown in Figure 7. We can find similar results from Figure 7 as from Figure 4; that is, for copolymers with branches shorter than $C_{10}H_{21}$, their crystallinity decreases with increasing branch length, whereas for copolymers having branches longer than $C_{10}H_{21}$, their crystallinity increases as the branch length increases. Further comparing the lamellar structures in Figure 7 with the corresponding structures in Figure 4, we can see that the lamellar structures in Figure 7 are more perfect. The results above can be confirmed by comparing the fractions of trans state in the corresponding lamellae obtained by isothermal and nonisothermal crystallization as shown in Figure 8. It can be easily seen that the fractions of trans state in lamellae obtained by nonisothermal crystallization have nearly

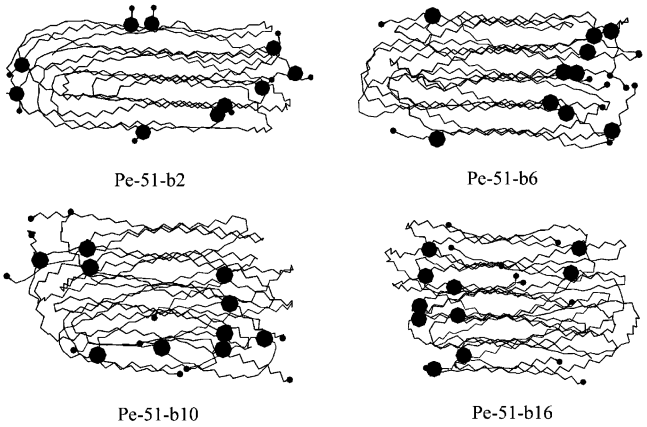


**Figure 7.** Lamellar structures of pe-51-b*n* ($n = 2$, 6, 10, or 16) chain models at $t = 15\,000$ ps, $T = 300$ K, where a large black sphere represents a branch site (CH unit) and a small one represents a branch termination group ($CH_3$ unit).

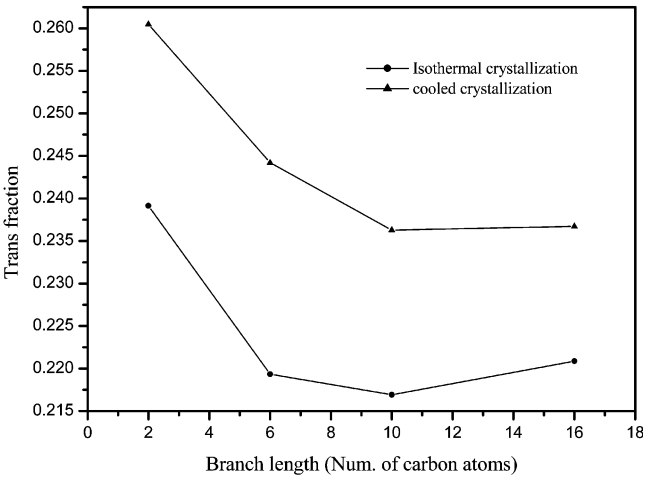


**Figure 8.** Fractions of trans state in the corresponding lamellae of pe-51-b*n* ($n = 2$, 6, 10, or 16) chains obtained by isothermal and nonisothermal crystallization.

the same variance trend as those obtained by isothermal crystallization. And it is obvious that the fractions of

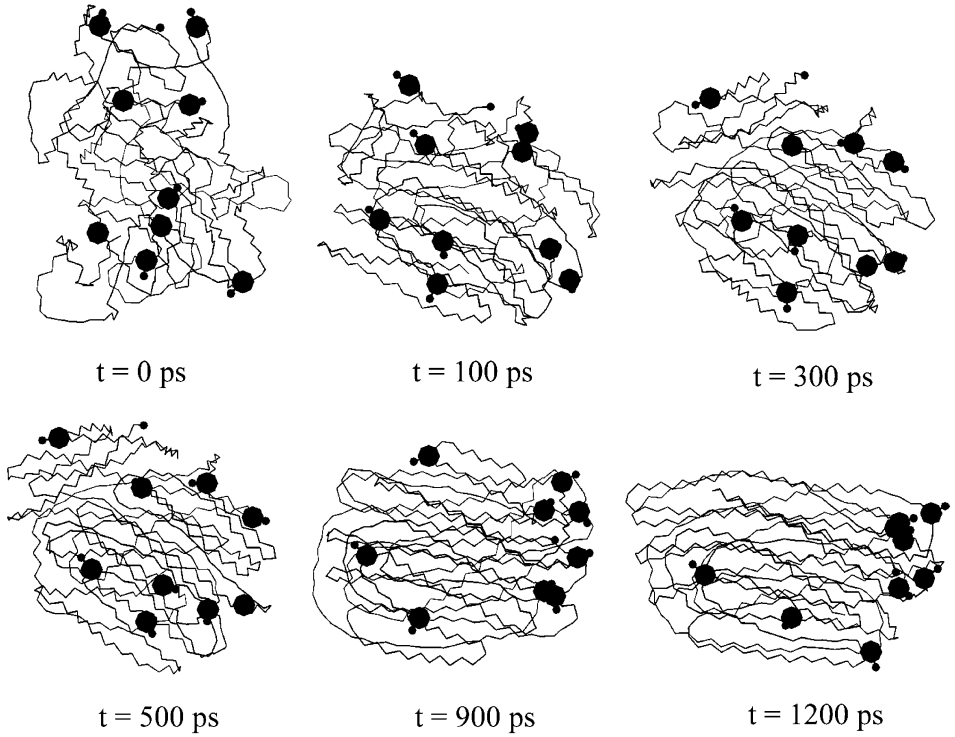


**Figure 9.** Collapse process of pe-51-cl chain starting from random coil at 300 K, where a large black sphere represents a branch site (CH unit) and a small one represents a chlorine atom.

trans state in lamellae obtained by nonisothermal crystallization are larger than those in the corresponding lamellae obtained by isothermal crystallization. Further studying Figures 2 and 6, we find that some local ordered domains are first formed near the branch sites, and then with these local domains coalescing to a lamellar structure the branch sites are rejected to the fold surface gradually. This process can be considered as crystal nucleation and growth at the early stage of copolymer crystallization. In nucleation the branch site acts as a nucleating seed, and in crystal growth the branch site is rejected from the crystal region as a defect.[35] In Figure 6, it is obvious that before a good lamellar structure is formed, most of the branch sites have been rejected to the boundary and most of the $CH_2$ segments are gathered into the crystal region; whereas Figure 2 shows that though a good lamellar structure has been formed, some branch sites still stay in the crystal region and some $CH_2$ segments stay at the boundary. So it is obvious that many more $CH_2$ segments are involved in the nonisothermal crystallization, which leads to the thicker lamella in the nonisothermally crystallized simulation. It should be noted that in this paper our main aim is to reveal the crystallization mechanism by theoretical method. Although the experimental observation for a cooling rate of 25 K/ns per step is difficult, we believe that our results may provide useful information for further experiments.

**C. Crystallization of LLDPE with Polar Comonomer.** To study the relaxation process of LLDPE with a polar comonomer, we show the relaxation process of pe-51-Cl chain starting from a random coil at 300 K in Figure 9, where the large black sphere represents a branch site (CH unit) and the small one represents a chlorine atom. Figure 9 shows that the relaxation process of the copolymer chain with polar branches is similar to that of the polymer chain with alkyl branches, that is, the adjacent sequences of trans bonds first aggregate together to form local ordered domains, and then they coalesce to a lamellar structure. In the process, the branch sites (CH units) and chlorine branches are rejected to the fold surface gradually.

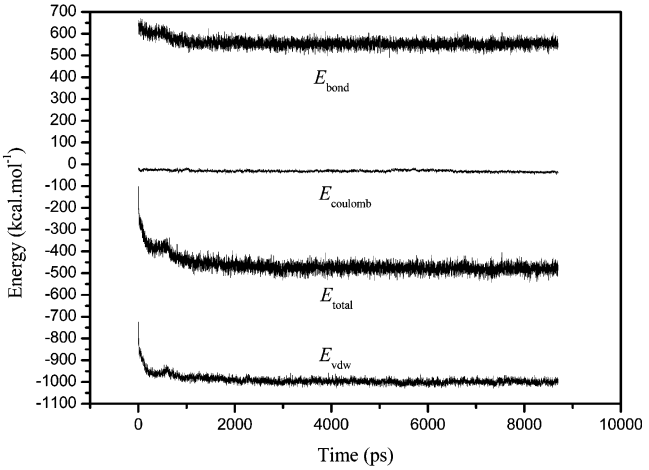


**Figure 10.** Time evolution of the bond, van der Waals, coulombic, and total potential energies of pe-51-cl chain.

Figure 10 shows the time evolution of the total potential, van der Waals, coulombic, and bond energies of the copolymer system. We can see that as the relaxation proceeds, the bond energy is repulsive (positive), while the van der Waals and coulombic energies are attractive (negative). Comparing the values of van der Waals energy with those of coulombic energy, we find that the coulombic interactions are relatively weaker. It is obvious that, during the relaxation process of pe-51-Cl chain, the total potential energy decreases due to the significant decrease of van der Waals energy. So for LLDPE with a polar comonomer as with a nonpolar α-olefin comonomer,[35] the main driving force for its collapse process is also the attractive van der Waals interaction between chain segments. From Figure

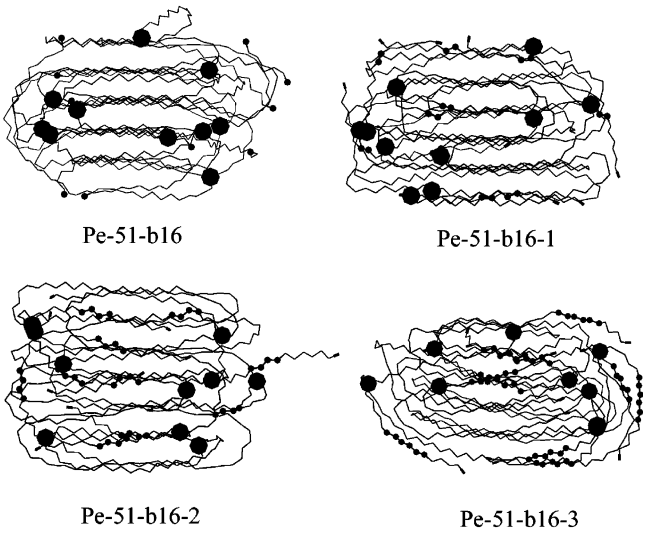


**Figure 11.** Conformations of pe-51-b16, pe-51-b16-1, pe-51-b16-2, and pe-51-b16-3 chains at $t = 8000$ ps, $T = 300$ K, where the one, two, and three double bonds in branches of pe-51-b16-1, pe-51-b16-2, and pe-51-b16-3, respectively, are represented by small black spheres. The short black line represents a $CH_3$ unit contained in the branch of the three copolymer chain models.

10 it can be seen that the fluctuation of the coulombic energy is rather small compared to the other energies, which may be because the QEq charge equilibration method is not periodically performed to redistribute the charges of the system during the MD simulation proceeding.

**D. Effect of Branch Flexibility on Side-Chain Crystallization.** It is known that when alkyl branches are sufficiently long, they will cocrystallize with the main chain of LLDPE. Russell et al.[41] reported experimentally that the minimum length of side chain to enter crystalline regions of ethylene/1-akene copolymers at 298 K is probably between 10 and 12 carbon atoms. In the experiment of Gerum et al.,[42] the critical length is reached in the case of hydrogenated poly[butadiene-*alt*-(1-dodecene)], which has branches with 10 carbons. Our previous[36] and present MD simulations show that when a branch is longer than $C_{10}H_{21}$, the branch will cocrystallize with the main chain. The simulation result is in harmony with the two experimental results.

As an extension, now let us study the effect of branch flexibility on side-chain crystallization. To study the effect of branch flexibility, we use models with different number of double C=C bonds but without including charges on the molecules, which is important to study the effect of unsaturation. In these models the more double bonds the stiffer the branch chain, and the effect of unsaturation may be ignored. Figure 11 shows the conformations of pe-51-b16, pe-51-b16-1, pe-51-b16-,2 and pe-51-b16-3 chains at $t = 8000$ ps, $T = 300$ K, where the one, two, and three double bonds in branches of pe-51-b16-1, pe-51-b16-2, and pe-51-b16-3 are represented by the small black spheres, and the short black line represents a $CH_3$ unit contained in the branch of the three copolymer chain models. From Figure 11, it can be seen that pe-51-b16-1, pe-51-b16-2, and pe-51-b16-3 copolymer chains formed lamellar structures. By comparing the three lamellae with that of pe-51-b16, it is found that the lamellar structure of pe-51-b16-1 (whose branch has one double bond) is more similar to that of pe-51-b16 chain. However, for pe-51-b16-2 and pe-51-b16-3 chains (whose branches have two and three double bonds, respectively), with the increasing double bonds, the corresponding lamella is packed more loosely, and more branches are rejected out from the crystal region. This means that as branch flexibility decreases, the side-chain crystallization becomes more difficult, and the stiffer branch prefers to stay out of the crystal region, which leads to the decreasing crystallinity of the copolymer. In Table 2 are listed the average total potential, bond, and van der Waals energies and radii of gyration of be-51-b16, pe-51-b16-1, pe-51-b16-,2 and pe-51-b16-3 chain systems. The time average is taken between 7500 and 8000 ps for each chain model. Comparing the values of $E_{vdW}$, $E_{bond}$, and $R_g$ of various copolymer chains, we find that with the increase in the number of double bonds in the branch, $E_{vdW}$ and $E_{bond}$ energies of the corresponding copolymer system decrease, whereas the corresponding $R_g$ increases. The result further illustrates that as branch flexibility decreases, the corresponding lamella is packed more loosely.

**Table 2. Time Averages of Potential Energies and Radius of Gyration for Copolymer Models with Branches of Different Flexibility**

| model | $E_{total}$ | $E_{vdW}$ | $E_{bond}$ | $R_g$ (Å) |
|---|---|---|---|---|
| pe-51-b16 | −526.07 | −1262.44 | 736.37 | 12.06 |
| pe-51-b16-1 | −532.29 | −1267.31 | 735.03 | 12.06 |
| pe-51-b16-2 | −530.01 | −1252.01 | 722.00 | 12.21 |
| pe-51-b16-3 | −519.81 | −1243.21 | 723.40 | 12.34 |

## IV. Conclusions

In this paper, we first study the effects of branch length and temperature on the crystallinity of LLDPE by MD simulations of the copolymer chain models with alkyl branches. The isothermal and nonisothermal crystallization processes of LLDPE chain are given. Furthermore, it is shown that for copolymers with branches shorter than $C_{10}H_{21}$, the crystallinity decreases with increasing branch length, whereas for copolymers having branches longer than $C_{10}H_{21}$, the crystallinity increases as the branch length increases. Then the crystallization of ethylene/polar monomer copolymer is simulated by use of an ethylene/vinyl chloride copolymer model. The simulation results show that the crystallization process and driving force of the LLDPE chain with a polar comonomer are similar to those with a nonpolar comonomer. Finally, the effect of branch flexibility on side-chain crystallization is investigated. It is found that as branch flexibility decreases, the side-chain co-crystallization becomes more difficult, and the stiffer branch prefers to stay out of the crystal region, which leads to the decreasing crystallinity of the corresponding copolymer.

**Acknowledgment.** This work is supported by the Natural Science Foundation of China (G29892168, 20073014), Doctor Foundation by the Ministry of Education, Foundation for University Key Teacher by the Ministry of Education, and Key Subject of Science and Technology by the Ministry of Education of China.

## References and Notes

(1) Mandelkern, L. *Crystallization of Polymers*; McGraw-Hill: New York, 1964.

(2) Kavassalis, T. A.; Sundararajan, P. R. *Macromolecules* **1993**, *26*, 4144.

(3) Sundararajan, P. R.; Kavassalis, T. A. *J. Chem. Soc., Faraday Trans.* **1995**, *91*, 2541.
(4) Liao, Q.; Jin, X. *J. Chem. Phys.* **1999**, *110*, 8835.
(5) Fujiwara, S.; Sato, T. *J. Chem. Phys.* **2001**, *114*, 6455.
(6) Fujiwara, S.; Sato, T. *J. Chem. Phys.* **1997**, *107*, 613.
(7) Liu, C.; Muthukumar, M. *J. Chem. Phys.* **1998**, *109*, 2536.
(8) Muthukumar, M.; Welch, P. *Polymer* **2000**, *41*, 8833.
(9) Koyama, A.; Yamamoto, T.; Fukao, K.; Miyamoto, Y. *J. Chem. Phys.* **2001**, *115*, 560.
(10) Yang, X.; Qian, R. *Macromol. Theory Simul.* **1996**, *5*, 75.
(11) Yang, X.; Mao, X. *Comput. Theor. Polym. Sci.* **1997**, *7*, 81.
(12) Guo, H. X.; Yang, X. Z.; Li, T. *Phys. Rev. E* **2000**, *61*, 4185.
(13) Yamamoto, T. *J. Chem. Phys.* **1998**, *109*, 4638.
(14) Yamamoto, T. *J. Chem. Phys.* **1997**, *107*, 2653.
(15) Zhang, X.; Li, Z.; Lu, Z. Sun, C. *J. Chem. Phys.* **2001**, *115*, 10001.
(16) ShiraYama, K.; Kita, S.; Watabe, H. *Makromol. Chem.* **1972**, *151*, 97.
(17) Culter, D. J.; Hendra, P. J.; Cudby, M. E. A.; Willis, H. A. *Polymer* **1977**, *18*, 1005.
(18) Wilfong, D. L.; Knight, G. W. *J. Polym. Sci. Part B: Polym. Phys.* **1990**, *28*, 861.
(19) Defoor, F.; Groeninckx, G.; Schouterden, P.; Van der Heijden, B. *Polymer* **1992**, *33*, 5186.
(20) Defoor, F.; Groeninckx, G.; Reynaers, H.; Schouterden, P.; Van der Heijden, B. *Macromolecules* **1993**, *26*, 2575.
(21) Lambert, W. S.; Phillips, P. J. *Macromolecules* **1994**, *27*, 3537.
(22) Lambert, W. S.; Phillips, P. J. *Polymer* **1996**, *37*, 3585.
(23) Gelfer, M. Y.; Winter, H. H. *Macromolecules* **1999**, *32*, 8974.
(24) Zhang, M.; Lynch, D. T.; Wanke, S. E. *J. Appl. Polym. Sci.* **2000**, 960.
(25) Alamo, R.; Domszy, R.; Mandelkern, L. *J. Phys. Chem.* **1984**, *88*, 6587.
(26) Burfield, D. R.; Kashiwa, N. *Macromol. Chem.* **1985**, *186*, 2657.
(27) Clas, S. D.; Mcfaddin, D. C.; Russell, K. E.; Scammell-Bullock, M. V. *J. Polym. Sci. Part A: Polym. Chem.* **1987**, *25*, 3105.
(28) Hosoda, S. *Polym. J.* **1988**, *20*, 383.
(29) Alamo, R. G.; Mandelkern, L. *Macromolecules* **1989**, *22*, 1273.
(30) Alamo, R. G.; Viers, B. D.; Mandelkern, L. *Macromolecules* **1993**, *26*, 5740.
(31) Kim, M.; Phillips, P. J. *J. Appl. Polym. Sci.* **1998**, *70*, 1893.
(32) Smith, J. A.; Brzezinska, K. R.; Valenti, D. J.; Wagener, K. B. *Macromolecules* **2000**, *33*, 3781.
(33) Watson, M. D.; Wagener, K. B. *Macromolecules* **2000**, *33*, 8963.
(34) Doran M.; Choi, P. *J. Chem. Phys.* **2001**, *115*, 2827.
(35) Zhang, X.; Li, Z.; Lu, Z.; Sun, C. *J. Chem. Phys.* **2001**, *115*, 3916.
(36) Zhang, X.; Li, Z.; Lu, Z.; Sun, C. *Macromolecules* **2002**, *35*, 106.
(37) Mayo, S. L.; Olafson, B. D.; Goddard, W. A., III. *J. Phys. Chem.* **1990**, *94*, 8897.
(38) Rappe, A. K.; Goddard, W. A., III. *J. Phys. Chem.* **1991**, *95*, 3358.
(39) Abu-sharkh, B.; Hussein I. A. *Polymer* **2002**, *43*, 6333.
(40) Aharoni, S. M.; Kramer, V.; Vernick, D. A. *Macromolecules* **1979**, *12*, 265.
(41) Russell, K. E.; Mcfaddin, D. C.; Hunter, B. K.; Heyding, R. D. *J. Polym. Sci. Part B: Polym. Phys.* **1996**, *34*, 2447.
(42) Gerum, W.; Höhne, G. W. H.; Wilke, W.; Arnold, M.; Wegner, T. *Macromol. Chem. Phys.* **1995**, *196*, 3797.

MA030010V